Towards LIDAR-RADAR based Terrain Mapping for Traversability Analysis

J.A. Guerrero, Marion Jaud, R Lenain, R Rouveure, P Faure

Towards LIDAR-RADAR based Terrain Mapping

J.A. Guerrero, M. Jaud, R. Lenain, R. Rouveure, P. Faure

***Abstract*— This paper addresses the problem of perception for autonomous vehicle navigation in real environments. Integrity safe navigation of autonomous vehicles in unknown environments poses a traversability problem. We are interested in the integrity-safe navigation in unknown environments. Safe navigation is a task that depends on the knowledge of the surrounding environment and the vehicle dynamics. Classical navigation approach focus on obstacle avoidance often based on occupancy and elevation maps. We propose to combine an optical sensor and an electromagnetic sensor to build a richer map of the environment which will be used for traversability analysis and path planning. The proposed lidar-radar map encodes the geometry of the environment such that traversability analysis and trajectory planning guarantee the robot's integrity in a stability sense. A comparative analysis of two mapping algorithms using lidar, radar, IMU and GPS sensors shows the advantages of such bimodal perception system. Results have been validated experimentally.**

I. Introduction

Development of autonomous robots involves the interaction of different domains such as modeling, control, path planning, terrain mapping, among others. In particular, terrain mapping and traversability analysis are key-features for autonomous robot navigation in unknown environments. As robots get more knowledge on the geometry of the terrain and the presence of static and dynamic obstacles, they can evolve in a way that the robot's integrity is guaranteed while minimizing the time to reach their goal.

Different approaches have been proposed in the literature for terrain mapping, [1], [2], [3], among others. There are mainly three approaches: 2D maps (occupancy), 2.5D maps (elevation) and 3D maps. The most common approach for terrain mapping is to project 3D data into a cartesian grid with some environment information (elevation, occupancy, traversability, etc.). Occupancy mapping [4] is one of the most utilized method for terrain mapping. Every cell in an occupancy map contains an occupancy probability which is used to determine if the cell is free, occupied or not explored. Alternatively, an elevation map is a 2D grid in which every cell contains height values of the terrain mapped. Elevation maps are also known as 2.5D maps. Similarly to the occupancy map, the computational requirements are not as important as for 3D mapping. An important disadvantage of 2.5D mapping is the fact that overhanging structures will be considered as obstacles. Depending on the data integration method used to update elevation information an elevation map fails to remove erroneous measurements since they do not handle uncertainty in sensor data. Recently a new data structure has been developed to model environment. This model consists in using an octree structure to divide the 3D space into small cubes. Tree-based representations such as octrees avoid one of the main shortcomings of grid structures by delaying the initialization of map volumes until measurements need to be integrated. Therefore, the size of the mapped environment does not need to be known beforehand. This representation seems to be memory efficient but not necessarily a good solution for real-time applications [5].

The interest of this paper is to present a method to create a rich terrain map which could be used to assess traversability for autonomous ground vehicles. In order to create terrain maps, on one hand, most approaches use information from stereo vision systems[6], 3D-lidar [7], and the coupling of a single camera and a single layer lidar [1]. 3D-lidar sensors usually provide a large point cloud of the environment. 3D lidar sensors based on 16 or more laser units are well suited for elevation and 3D mapping which can be used in the traversability analysis of the terrain. However, their perception performance is highly dependent on good weather conditions. On the other hand, microwave radar provides a single layer occupancy of the environment and seems to be able to take up the challenge of perception in outdoor environment, covering a long range, allowing rapid collection of data and overcoming the limitations of vision-based sensors affected by ambient lighting conditions, rain, dust, fog, snow, etc. [8], [9]. In this work, we propose to exploit the advantages of lidar and radar sensors shown in Figure 1 to create a robust mapping system. The combination of both optical and microwave sensors would provide a richer map that can be used for traversability analysis of mobile robots.

This work is organized as follows: section II describes a method used to build an occupancy map using a RADAR sensor. Section III presents a method to characterize the environment into 2.5D and intensity-based maps. Section IV presents a multi-sensor approach to create a rich feature terrain map. The final map is computed by integrating both radar-only and lidar-only maps into a GIS (Geographic Information System). Experimental setup and results are discussed in section V. Conclusions and perspectives are finally given in Section VI.

J.A. Guerrero (jguerrer@ieee.org) is with the LITIS laboratory, INSA de Rouen, Saint Etienne de Rouvray, France. M. Jaud is with (marion.jaud@univ-brest.fr), Laboratoire Domaines Océaniques (UMR 6538), Université de Bretagne Occidentale, Brest, France. R.Lenain, R. Rouveure and P. Faure (roland.lenain, raphael.rouveure, patrice.faure @irstea.fr) are with the IRSTEA laboratory. 9 Ave. Blaise Pascal, Aubière, France.

Fig. 1. (left) PELICAN radar, (right) Velodyne lidar

II. Radar-only Mapping

The PELICAN radar uses the Frequency Modulated Continuous Wave (FMCW) principle as described in details in [8] and [10]. The radar range is 100 m with a transmitted power about 50 mW, antenna gain of 20 dB and carrier frequency of 24 GHz. Waves are emitted through an antenna (aperture angle 20° vertical, 5° horizontal) rotating in horizontal plane, so that a strip of ground perpendicular to the vehicle displacement plane is illuminated (Fig. 2).

A portion of the emitted wave is reflected back towards the radar antenna. Following the FMCW radar theory, the radar target distance is computed from the beat frequency [11]. A signal of linearly increasing frequency is transmitted via the antenna. The transmitted signal is mixed with the signals received from the targets, giving the beat signal S_b. The beat signal S_b is the sum of i frequency components $f_b i$, each of them corresponding to a particular target [10], [11]:

$$f_{bi} = 2\Delta f f_m \frac{r_i}{c} + 2f_0 \frac{v_i}{c} \quad (1)$$

where f_0 is the carrier frequency, f_m the modulation frequency and Δf the frequency scan. The beat frequency is proportional to the target distance r_i, and on the radial velocity v_i.

The power of the received signal depends on the characteristics of the target i.e. its Radar Cross Section (RCS) which describes the ability of the target to reflect the radar wave. The PELICAN radar achieves a complete 360° scan in one second. An image is built up from the successive angular scans recorded during the antenna rotation (Fig. 2). A 360° radar scan in the horizontal plane leads to a polar image built up from radar-target distances measured by FFT techniques at each step of antenna rotation in the horizontal plane. The distance and the angular resolution in the polar image are respectively about 1 m and 5°. As described in Fig. 3, at the end of a complete antenna scan, the intra-scan distortions due to vehicle motion during antenna rotation are corrected and the speckle is filtered. The 1025 x 1025 pixel image computed from power spectrum measurement at each degree of antenna rotation is called "panoramic radar image".

The global map is built by iteration through the association of successive panoramic radar images thanks to the "R-SLAM algorithm" [8]. This algorithm is based on the Simultaneous Localization and Mapping (SLAM) process,

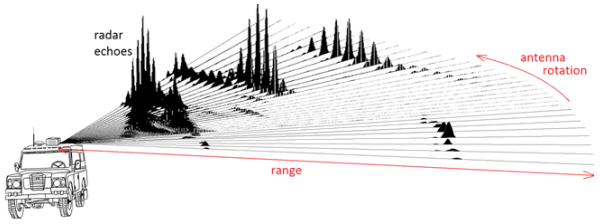

Fig. 2. Radar-based intensity map

widely used in mobile robotic, by which a mobile sensor can build a relative map of its environment and simultaneously computes its relative location within the map [12], [13]. As it can be seen in Fig. 3, a 3D cross-correlation is performed between the n^{th} radar panoramic image and the previously constructed map, on one hand in order to match them, updating the global radar map and on the other hand in order to estimate the radar inter-scan displacement and rotation. The radar map is so computed independently of the platform dynamics and of the radar position on the vehicle.

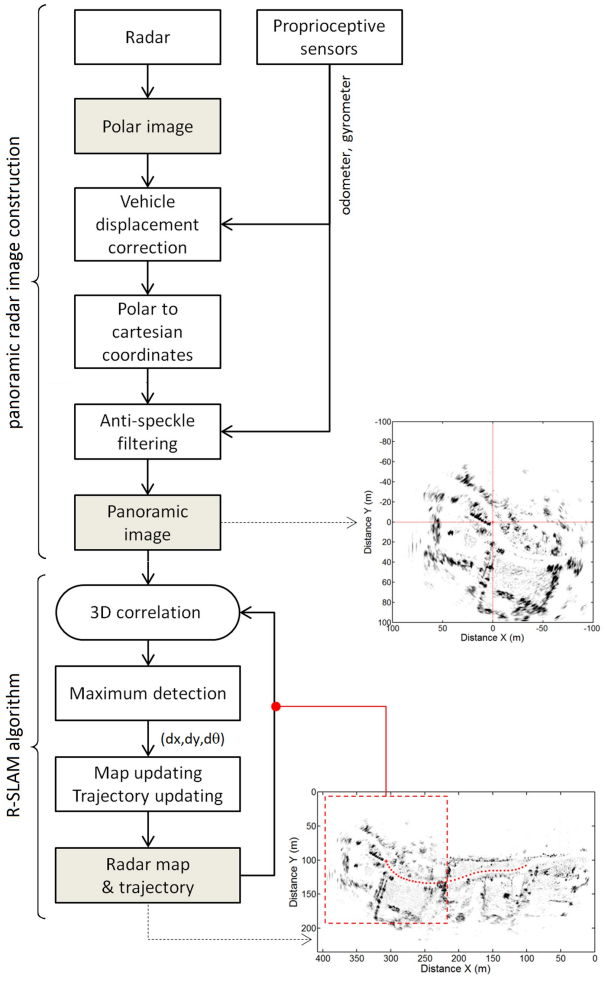

Fig. 3. Radar-based intensity map

The final radar map is a gray-scale raster, with a spatial resolution of 20 cm. The gray-scale level results from the

amplitude of the reflected echoes from environment. Considering successive inter-scan displacements and rotations, the relative radar trajectory (named "R-SLAM trajectory") is computed simultaneously. Figure 4 shows the final map using the R-SLAM algorithm.

The global map is finally georeferenced either by taking advantage of GPS recording or by manual or automatic matching to an orthophotograph, as described in [14].

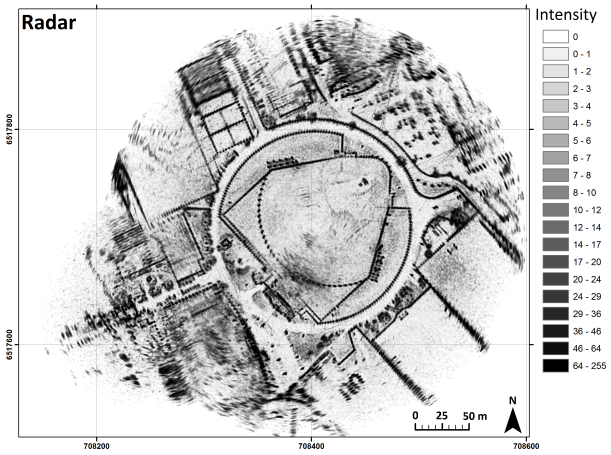

Fig. 4. Radar-based intensity map

III. Lidar-only Mapping

The most common 3D sensors are the RGBD cameras and 3D lidar scanners (e.g. SICK, Velodyne, etc.). RGBD cameras have a short perception range, often inferior to 10m, and a limited field of view (FoV), however they have a high resolution resulting in a high density point clouds with color, range and intensity information. 3D laser scanners have a long perception range, usually larger than 30m, a wide scan range $(270^\circ - 360^\circ)$ FoV and low resolution resulting in a point cloud with range and intensity data. Our vehicle is equipped with a GPS RTK, a nine-degree-of-freedom inertial measurement unit (IMU) sensor and a 32 layer velodyne lidar sensor which provides around 700000 range-reflectance measurements/second.

In order to create a model of the environment using 3D scanners there are different methods that can be found in the literature. A widely used method for scan matching is the Iterative Closest Point (ICP) method [15]. ICP has proven to be efficient for scan matching using RGBD cameras and some range scanners in feature rich environments, and real time implementations have been proposed in [16], [18]. On one hand, it is is important to mention that most of existing results in terrain mapping using ICP have been used in urban feature rich environments. On the other hand, it is clear that the main weakness of ICP is their feature dependent nature. Our experimental tests on Velodyne-type data have shown a poor performance in presence of few obstacles and symmetrical scenarios since ground points close to the sensor are dominant with respect to obstacles at mid and long range as shown in Figure 5. Notice that, in Fig 5-(d), ICP method result in a poor rotation convergence. Moreover, it is clear that ICP was unable to converge to the actual translation of the sensor. In addition, [17] presents a discussion of the impact of the geometry of the data on the performance and convergence of the ICP method. The authors have shown that ICP does not guarantee the convergence of registration process in symmetrical scenarios and smooth (few features/obstacles) scenarios. Since we are interested in creating a mapping process to analyse the traversability of a terrain in all kind of environments (urban and off-road), ICP method is not suitable for our application.

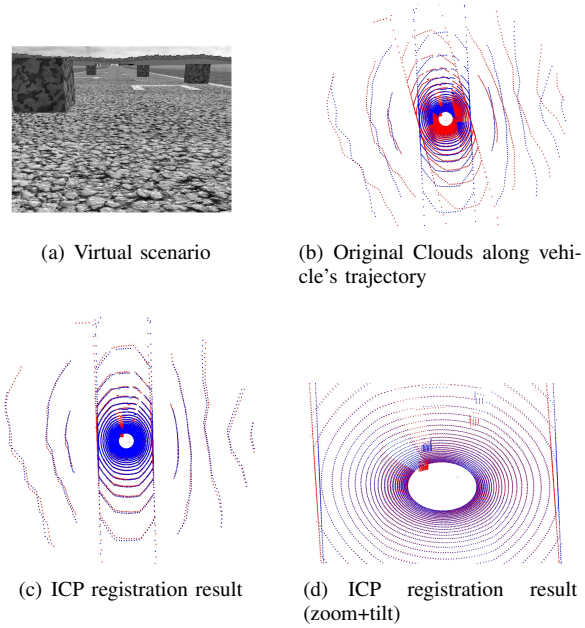

(a) Virtual scenario

(b) Original Clouds along vehicle's trajectory

(c) ICP registration result

(d) ICP registration result (zoom+tilt)

Fig. 5. Unstable geometry. ICP results in objects moving towards the vehicle rather than converging to the vehicle's translation

The purpose of the lidar mapping process is to provide the vehicle with a real-time terrain reconstruction module, particularly at high velocities. The traversability analysis requirements for a ground robot impose the creation of terrain model that describes the geometry of the surface, the presence of obstacles, etc. To do so, 2.5D and occupancy maps are suitable for real-time applications. Since the lidar sensor provides a large amount of data that needs to be registered into a map (elevation, occupancy, etc.). Instead of using a SLAM approach that could slow down the mapping process, which may limit the maximal vehicle's velocity to guarantee the real-time mapping process, the GPS and IMU sensors are used to determine the vehicle's position. Notice that the position of the vehicle is estimated using a Kalman filter. Roll and pitch angles have been estimated using the information of the accelerometers and gyrometers of the IMU. The attitude of the vehicle is computed using a complementary filter described in [19].

The heading angle is estimated via a state reconstruction based on a Kalman filter [20]:

$$\bar{\theta}_k = \hat{\theta}_{k-1} + \frac{vT}{l}\tan(\delta_k) \quad (2)$$

$$\hat{\theta}_k = \bar{\theta}_{k-1} + L(\theta_k^m - \bar{\theta}_k) \quad (3)$$

where θ is the heading angle, v is the vehicle's velocity, T is the sampling period, δ is the front steering angle, L is the scalar Kalman gain, θ_k^m is the measured heading angle and $\hat{\theta}$ is the estimated heading angle to bue used in the registration process.

Once position and attitude have been computed, the point clouds can be registered and integrated into a local map using a rigid transformation with respect to the global initial position of the robot. The elevation at a given cell is fairly estimated as the average of the points within that cell. Integrating multiple measurements is useful to cope with the blind spots of a given sensor. The cell resolution has been set to 20 cm to meet the same resolution of the radar-only map method. Every cell contains multiple features of the environment, elevation, reflectance, occupancy, among other. The main advantage of this approach is that the terrain map module is capable of running in real-time without losing information from sensors making of it a potential solution for terrain traversability analysis. A drawback of this approach is the implicit assumption that the full 360° scan is acquired instantaneously. It is worth to mention that the Velodyne sensor is a rotating lidar rangefinder and therefore vehicle displacement correction should be applied mainly in turning operations. In practice, we noticed that the distortion due to vehicle translation is not as significative as for the radar sensor. This is due to the fact that lidar sampling frequency is 10 times higher than the radar sampling frequency. Figure 6 shows the final map (mean of intensity values) using the proposed algorithm.

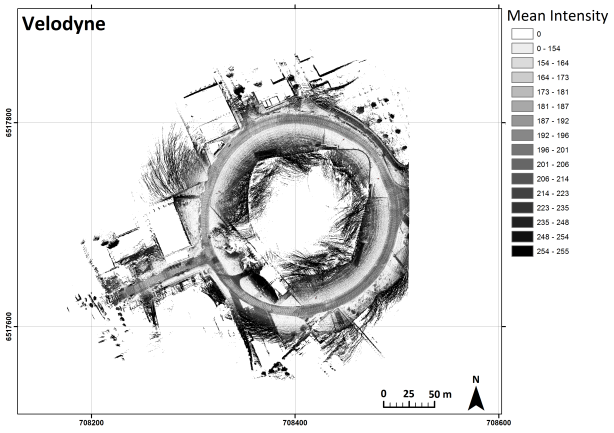

Fig. 6. Lidar-based intensity map

IV. Multi-sensor approach

Since each sensor provides different information about the environment, we opted for integrating the information into a single map with multiple features (occupancy, elevation, optical reflectance, magnetic reflectance, etc.). Although a 3D lidar sensor allow us to create both occupancy and elevation maps, its performance highly depends on weather conditions. On the other hand, although a radar-based sensor can only be used to create occupancy maps, it can be used in almost any weather condition. Thus, we propose to fuse both maps (lidar-based and radar-based) to obtain an improved mapping system.

Since each sensor provides intrinsically different information about the environment, it is a delicate issue to define a unique indicator merging all the collected information. Therefore, we opted for an approach similar to a GIS and geographical database. GIS is a tool widely used in geographical science since it allows to store, manage and analyze all types of objects defined in a geometric space. Different attributes characterize these objects, for example in our case: occupancy, elevation, optical reflectance, magnetic reflectance, etc. The storing structure consists of "classes" of spatial objects, each of them implemented by a layer.

Both lidar and radar maps are projected in the same reference system so that each pixel of the lidar map is coincident with the equivalent pixel of the radar map. Lidar map is directly georeferenced, exploiting IMU and GPS recordings. The projection of the radar map has been achieved by matching the R-SLAM trajectory and the GPS RTK trajectory. The matching processus consists on using the R-SLAM trajectory as tie points which are match with the GPS RTK trajectory to compute an affine transformation.

$$\begin{pmatrix} u \\ v \end{pmatrix} = \begin{pmatrix} A & B & C \\ D & E & F \end{pmatrix} \begin{pmatrix} x \\ y \\ 1 \end{pmatrix} \quad (4)$$

where A, E are the scale factors (size of pixel in map units in x- and y-direction), B, D are rotation terms and C, F are the translation terms for the upper left pixel in geographic coordinates These terms are unknowns to be computed. The accuracy of this georeferencing method is about 10 cm [14], i.e. lower than spatial data resolution. All data are georeferenced in Lambert 93, the French official coordinate system, based on GRS 80 ellipsoid. Thus, information collected by both systems is compiled in a single map composed of several layers. In this way, the multi-layer structure enables to retrieve all the information about a location performing a "spatial query", i.e. for a given pixel or a given area, we can access the information collected by both system. In this paper the multi-layer maps are implemented with ArcGIS© software, but they can be easily exported to other software tools (Matlab©, Effibox©, etc.).

V. Experimental Setup and Results

A. Experimental platform

In order to validate our discussion, an experimental vehicle has been equipped with the following sensors: GPS RTK, Xsens IMU, Pelican radar, and Velodyne lidar. The following table presents a comparison of the mapping sensors used in this work.

The acquisition-piloting software and the previously described processing chain for radar-only mapping have been

TABLE I

COMPARISON OF MAIN CHARACTERISTICS

Feature	Pelican radar	Velodyne lidar
Range	100 m	70 m
Angular Resolution	5°	0.16°
Distance Resolution	1m	variable
Vertical Resolution	$--$	1.33°
Scan Freq.	1Hz	10Hz
Accuracy	2 cm	< 2 cm
Size	27 x 24 x 30 cm	15 x 8.6 x 8.6 cm
Weight	10 kg	1 kg
Weather conditions	Wide (fog, night, etc.)	Clear weather

TABLE II

AFFINE TRANSFORMATION PARAMETERS

Parameter	radar	lidar
A	0.1786	0.2021
B	0.0879	-0.0009
C	708064.1951	708147.5527
D	0.0893	-0.0012
E	-0.1779	-0.1996
F	6517760.9349	6517906.9895

developed in Matlab©, independently of multi-sensor fusion perspectives. Thus, the R-SLAM method had been chosen because in this way, there is no need of inertial measurement unit (IMU) sensor. It should be noticed that the RADAR-only mapping data acquisition architecture has been designed for mapping applications. Thus the occupancy map has been computed off-line due to computational issues. LiDAR-only mapping has been computed in real-time using Effibox, a data acquisition software similar to the well known Robotic Operative System (ROS). A terrain map library in C language has been adapted for usage with Effibox middleware. Notice that the data acquisition systems are based in different architectures since they have been designed for different applications. Then, the feature rich map has been computed off-line such that the final map is independent of the acquisition system. The architecture for terrain mapping is depicted in Figure 7. Notice that the GIS module is assumed to be able to respond to spatial queries from the vehicle control module via the robotic middleware Effibox. The affine transformation for each map as been computed as

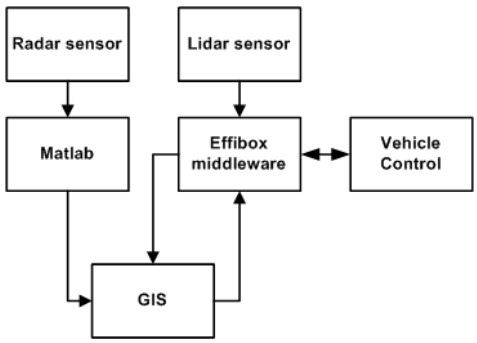

Fig. 7. Lidar-radar mapping architecture

B. Scenario selection

We have chosen a roundabout around a baseball field at Clermont-Ferrand as the experimental site. The experimental site includes large buildings, the presence of vehicles parked along the selected road, the presence of pedestrians and athletes, large flat obstacle free sections (baseball field), and trees. The vehicle's velocity has been set to 6m/s. Figure 8 shows the global map georeferenced of lidar-only mapping (top), radar-only mapping (center) and the combined lidar-radar map (bottom).

From Figure 8, it is clear that both sensors and the mapping methods described above produce similar results. A qualitative correspondence of the lidar and radar maps can be observed in Figure 8 (bottom). It is clear that the radar sensor correctly detects the metallic posts of the baseball batting cage shown in Figure 9 while it fails to detect the nylon net. On the other hand, the lidar sensor correctly detects both the metallic posts and the nylon net.

VI. CONCLUDING REMARKS AND FUTURE WORKS

In this paper, we have presented two terrain mapping methods using two different sensors with similar operation mode. The Radar-only method computes the terrain map offline using R-SLAM. The lidar-only map is computed online using a classical kalman filter. An integration of lidar and radar maps has been implemented to build an information rich map for autonomous navigation purposes. The new map includes information such as elevation, occupancy and reflectance. The final map includes multiple layers that can be retrieved using spatial queries to a GIS. A library in C language has been developed to compute the lidar-only mapping in real-time. Since the data acquisition chains for each sensor are based in different software (Matlab DAQ and Effibox (C/C++)), future work includes developing a unified data acquisition system in a robotic middleware such as Effibox or ROS. Similarly, we aim to extract features from the terrain map for terrain traversability analysis using either a non supervised or a semi-supervised classification approach.

REFERENCES

[1] F. Malartre, T. Feraud, C. Debain, R. Chapuis, "Digital Elevation Map Estimation by Vision-Lidar Fusion", In *Intl. Conf. on Robotics and Automation (ICRA)*, China, 2009.

[2] A. Souza, R.S. Maia, R.V. Aroca, L.M.G. Goncalves, "Probabilistic Robotic Grid Mapping based on Occupancy and Elevation Information", In , , 2013.

[3] A. Broggi, E. Cardarelli, S. Cattani, M. Sabatelli, "Terrain Mapping for Off-road Autonomous Gound Vehicles Using Rational B-Splines Surfaces and Stereo Vision", In *IEEE Intelligent Vehicles Symposium*, Australia, 2013.

[4] A. Elfes, "Sonar-based real-world mapping and navigation", Journal of Robotics and Automation, Vol. 3, No. 3, pp.249-265, 1987.

[5] K.M. Wurm, A. Hornung, M. Bennewitz, C. Stachniss, W. Burgard, "OctoMap: A Probabilistic, Flexible, and Compact 3D Map Representation for Robotic Systems", 2010.

[6] G. De Cubber, D. Doroftei, L. Nalpantidis, G.Ch. Sirakoulis, A. Gasteratos,"Stereo-based Terrain Traversability Analysis for Robot Navigation", IARP/EURON Workshop on Robotics for Risky Interventions and Environmental Surveillance, 2008.

[7] J. Larson, M. Trivedi, M. Bruch, "Off-road Terrain Travesability Analysis and Hazard Avoidance for UGVs", IEEE Intelligent Vehicles Symposioum, 2011.

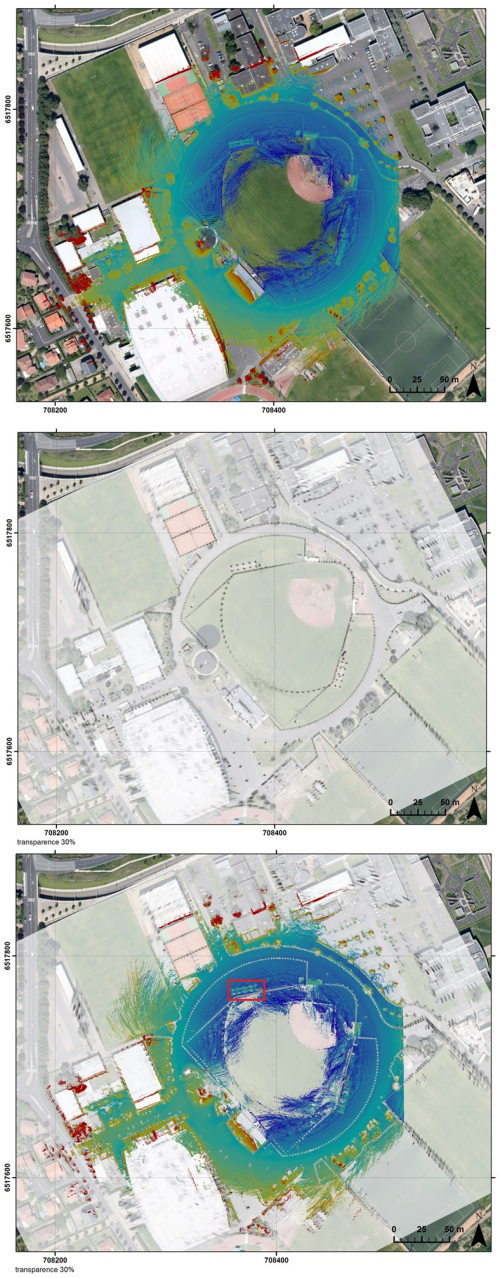

Fig. 8. (Top) lidar-only map, (center) radar-only map, (down) Lidar-radar map

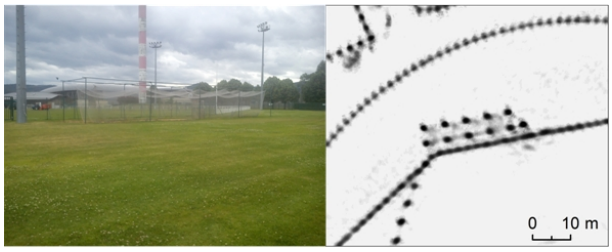

Fig. 9. Baseball batting cage located in red square section of final map

[8] R. Rouveure, M-O. Monod, and P. Faure, "Mapping of the environment with a high resolution ground-based radar imager", IEEE International Conference on Radar Systems RADAR'09, pp.822-828, 2009.

[9] Peynot, T., Scheding, S., Terho, S., "The Marulan Data Sets: Multi-Sensor Perception in Natural Environment With Challenging Conditions". The International Journal of Robotics Research 29 (13), 1602-1607, 2010.

[10] M-O. Monod, "Frequency modulated radar: a new sensor for natural environment and mobile robotics". Ph.D. Thesis, Paris VI University, France, 1995.

[11] M.I. Skolnik, "Introduction to radar systems," in Electrical Engineering Series, McGraw-Hill International, Eds. New-York, 1980.

[12] Durrant-Whyte, H., Bailey, T., "Simultaneous localization and mapping: part I", IEEE Robotics and Automation Magazine 13 (2), 99-108, 2006.

[13] Bailey, T., Durrant-Whyte, H., "Simultaneous localization and mapping (SLAM): part II", IEEE Robotics and Automation Magazine 13 (3), 108-117, 2006.

[14] M. Jaud, R. Rouveure, P. Faure, and M-O. Monod, "Methods for FMCW radar map georeferencing", ISPRS Journal of Photogrammetry and Remote Sensing, vol. 84, pp. 33-42, October 2013.

[15] M. Levoy, S. Rusinkiewicz, M. Ginzton, J. Ginsberg, K. Pulli, D. Koller, S. Anderson, J. Shade, B. Curless, L. Pereira, J. Davis and D. Fulk, "The Digital Michelangelo Project: 3D Scanning of Larges Statues", in Proc. of Computer Graphics (SIGGRAPH), 2000.

[16] S. Rusinkiewicz, and M. Levoy, "Efficient Variants of the ICP Algorithm", Intl. Conf. on 3-D Digital Imaging and Modeling, 2001.

[17] N. Gelfand, L. Ikemoto, S. Rusinkiewicz, and M. Levoy, "Geometrically Stable Sampling for the ICP Algorithm", Fourth International Conference on 3D Digital Imaging and Modeling, 2003.

[18] F. Pomerleau, P. Krusi, F. Colas, P. Furgale, and R. Siegwart, "Long-term 3D map maintenance in dynamic environments", IEEE Conf. on Robotics and Automation (ICRA), 2014, pp. 3712-3719.

[19] R. Mahony, T. Hamel, J.M. Pflimlin, "Non-linear Complementary Filters on the Special Orthogonal Group", IEEE Trans. on Automatic Control, Vol. 53, No. 5, 2008.

[20] B. Thuilot, C. Cariou, L. Cordesses, P. Martinet, "Automatic Guidance of a Farm Tractor Along Curved Paths using a unique CP-DGPS", IEEE Intl. Conf. on Intelligent Robots and Systems, 2001.

[21] S. Lacroix, I-K. Jung, A. Mallet, "Digital Elevation Map Building from Low Altitude Stereo Imagery", Robotics and Autonomous Systems, Vol. 41, No. 2-3, Pages 119-127, 2002.